FREQUENCY-DEPENDENT WAVE EQUATION TRAVELTIME INVERSION

YIBO WANG[1], YIKANG ZHENG[1,2], XU CHANG[1] and ZHENXING YAO[3]

[1] *Key Laboratory of Engineering Geomechanics, Institute of Geology and Geophysics, Chinese Academy of Sciences, 19 Beitucheng Xilu, Chaoyang District, Beijing 100029, P.R. China. wangyibo@mail.iggcas.ac.cn*
[2] *University of Chinese Academy of Sciences, Beijing 100049, P.R. China.*
[3] *Division of the Earth's Deep Structure and Process, Institute of Geology and Geophysics Institute of Geology and Geophysics, Chinese Academy of Sciences, Beijing 100029, P.R. China.*

(Received January 27, 2014; revised version accepted July 7, 2014)

ABSTRACT

Wang, Y., Zheng, Y., Chang, X. and Yao, Z., 2014. Frequency-dependent wave equation traveltime inversion. *Journal of Seismic Exploration*, 23: 367-378.

We demonstrate the cross-correlation based traveltime residuals estimated from band limited seismic data vary according to the components in the frequency band, and propose a method to invert such frequency dependent traveltime residuals for velocity inversion. The proposed inversion algorithm is based on the wave equation and is referred to as FWT (frequency dependent wave equation traveltime inversion). In the proposed method, we start the inversion using cross-correlation based traveltime residuals estimated within low frequency data, followed by the inversion at higher frequencies. The effectiveness and performance of the FWT method is demonstrated by using a synthetic cross-well dataset. The numerical results show that the FWT yields improved results compared to those resulted from the conventional wave equation traveltime inversion (WT) approach, and FWT is more suitable to be the initial velocity model for the subsequent high resolution velocity inversion, e.g., full waveform inversion.

KEYWORDS: traveltime inversion, wave equation, frequency-dependent, crosswell, FWT.

INTRODUCTION

Accurate velocity model building is a key component for obtaining high resolution subsurface image of complex oil and gas reservoirs. There are various seismic velocity inversion methods that can be roughly divided into two major categories: a) traveltime inversion (Dines and Lytle, 1979; Bishop et al., 1985;

0963-0651/14/$5.00

Ivansson, 1985; Paulsson et al., 1985; Luo and Schuster, 1991) and, b) full waveform inversion (Tarantola, 1986; Mora, 1987; Crase et al., 1992). Both methods have strong and weak points and in general can be viewed as complementary to each other. Full waveform inversion (FWI) can provide the most accurate and high-resolution velocity model (Tarantola, 1984). However, the problem of FWI is that its misfit function can be highly nonlinear with respect to the initial velocity model (Gauthier et al., 1986), and thus the inversion procedure tends to have problems with local minima if the starting model is not in the vicinity of the actual one. Wave-equation traveltime inversion (WT) minimizes traveltime residuals (Luo and Schuster, 1991; Zhou et al., 1995; Zhang et al., 2011). In WT, the misfit function depends on the time lag of maximum cross-correlation between the observed and modeled data and is quickly converging even if the starting model is not close to the actual one. Moreover, the reconstructed velocity model has a relatively high resolution and can be used as a good initial model for subsequent FWI applications (Shen et al., 2012).

In this paper, we first examine the basic theoretical concepts of the WT. We then demonstrate that the cross-correlation based traveltime residuals are frequency dependent and propose a new frequency dependent wave-equation traveltime inversion method, named FWT. We employ a synthetic cross-well dataset to apply and validate the proposed methodology. The obtained numerical results show that FWT can partly eliminate the local minima issues encountered in WT. Furthermore, FWT provides a much improved initial velocity model for further FWI procedures compared to WT.

METHODOLOGY

Wave-equation traveltime inversion (WT)

The time domain acoustic wave equation can be expressed as following

$$[1/c^2(\mathbf{r})][\partial^2 P(\mathbf{r},t|\mathbf{r}_S)/\partial t^2] - \rho(\mathbf{r})\nabla\cdot\{[1/\rho(\mathbf{r})]\nabla P(\mathbf{r},t|\mathbf{r}_S)\} = S(t|\mathbf{r}_S) \quad , \quad (1)$$

where $P(\mathbf{r},t|\mathbf{r}_S)$ is the pressure field at position $\mathbf{r}$ and t denotes time. $S(t|\mathbf{r}_S)$ is the source function at location $\mathbf{r}_S$, $c(\mathbf{r})$ is the velocity and $\rho(\mathbf{r})$ is the density.

The misfit function of wave-equation traveltime inversion is defined as following

$$F(c) = \tfrac{1}{2} \sum_s \sum_g [\Delta\tau(\mathbf{r}_g|\mathbf{r}_s)]^2 \quad , \quad (2)$$

where $\Delta\tau$ is the traveltime difference between the observed and calculated seismograms.

The traveltime difference $\Delta\tau$ can be obtained by maximizing the following cross-correlation function (Luo and Schuster, 1991)

$$f(\mathbf{r}_g,\Delta\tau|\mathbf{r}_s) = [P_{obs}(\mathbf{r}_g,t+\Delta\tau|\mathbf{r}_s)/A_{obs}(\mathbf{r}_g|\mathbf{r}_s)]P_{cal}(\mathbf{r}_g,t|\mathbf{r}_s) \quad , \tag{3}$$

where $A_{obs}(\mathbf{r}_g|\mathbf{r}_s)$ is the maximum amplitude of $P_{obs}(\mathbf{r}_g,t|\mathbf{r}_s)$.

To update the velocity model, several optimization methods can be used. In the simplest case, a steepest descent method based velocity updating equation is given by

$$c_{k+1}(\mathbf{r}) = c_k(\mathbf{r}) + \alpha_k\gamma_k(\mathbf{r}) \quad , \tag{4}$$

where α_k is the velocity updating step length which is determined by a line-search method. The γ_k is the steepest descent direction and can be calculated using the equation as follows:

$$\gamma_k(\mathbf{r}) = [1/c^3(\mathbf{r})]\sum_s\sum_t \dot{P}_{cal}(\mathbf{r},t|\mathbf{r}_s)\dot{P}'(\mathbf{r},t|\mathbf{r}_s) \quad , \tag{5}$$

where $P'(\mathbf{r},t|\mathbf{r}_s) = \Sigma_g G(\mathbf{r}|\mathbf{r}_g) * \delta\tau(\mathbf{r}_g,t|\mathbf{r}_s)$. The symbol $*$ represents temporal convolution, $\dot{P}$ represents the time derivative of P, and $G(\mathbf{r}|\mathbf{r}_g)$ is the Green's function associated with eq. (1). The $\gamma_k(\mathbf{r})$ is the inner product of observed P and the back propagated pseudo travel-time residual, which is defined by

$$\delta\tau(\mathbf{r}_g,t|\mathbf{r}_s) = -(2/E)\dot{P}_{obs}(\mathbf{r}_g,t+\Delta\tau|\mathbf{r}_s)\Delta\tau(\mathbf{r}_g|\mathbf{r}_s) \quad , \tag{6}$$

and the normalization factor E is given as

$$E = \int \dot{P}_{obs}(\mathbf{r}_g,t+\Delta\tau|\mathbf{r}_s)\dot{P}_{cal}(\mathbf{r}_g,t|\mathbf{r}_s)dt \quad . \tag{7}$$

Frequency dependent wave-equation travel-time inversion (FWT)

The gradient $\gamma_k(\mathbf{r})$ in eq. (5) can be written as follows

$$\gamma_k(\mathbf{r}) = -[2/Ec^3(\mathbf{r})]\sum_s\sum_t K\Delta\tau(\mathbf{r}_g|\mathbf{r}_s) \quad , \tag{8}$$

where K represents the sensitivity kernel and is defined as follows

$$K = \dot{P}_{cal}(\mathbf{r},t|\mathbf{r}_s)\Big(\sum_g G(\mathbf{r}|\mathbf{r}_g) * \dot{P}_{obs}(\mathbf{r}_g,t+\Delta\tau|\mathbf{r}_s)\Big) \quad . \tag{9}$$

Here, $\dot{P}_{cal}$ and $\dot{P}_{obs}$ represent the time derivative of P_{cal} and P_{obs}, respectively. We will demonstrate that for the gradient $\gamma_k(\mathbf{r})$, the cross-correlation based travel-time difference $\Delta\tau$ is frequency dependent. The basic idea is to decrease the local minima by decomposing the seismic data to different scales. As the cross-correlation based traveltime differences are changed with the increasing peak frequency of source wavelet, the inversion result will be improved at increasing frequencies. At low frequency, the local minima are greatly reduced and the global minima are more likely to be obtained. FWT uses the result at the low frequency as an initial model at higher frequencies and update the model recursively.

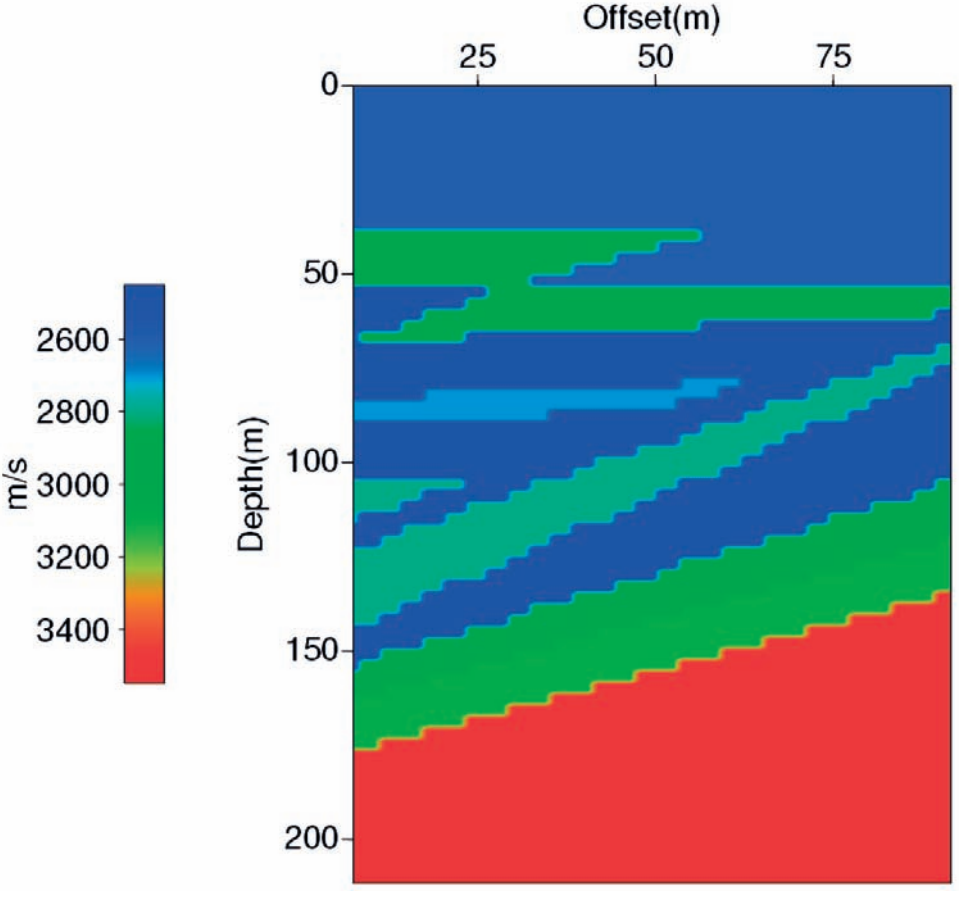

Fig. 1. A true velocity model with faults inside.

Fig. 1 exhibits a fault velocity model while Fig. 2 depicts its smoothed version. We define the window size in the depth and offset directions and then smooth the velocity or slowness, via a damped least squares technique. Here the window size we choose is $r_1 = 30$ in the depth direction and $r_2 = 15$ in the offset direction. Both models contain 142 grid points vertically and 62 grid points horizontally. The grid interval is 1.5 m in both horizontal and vertical directions. The two models are employed to demonstrate that the cross-correlation based traveltime differences calculated from Figs. 1 and 2 are frequency dependent.

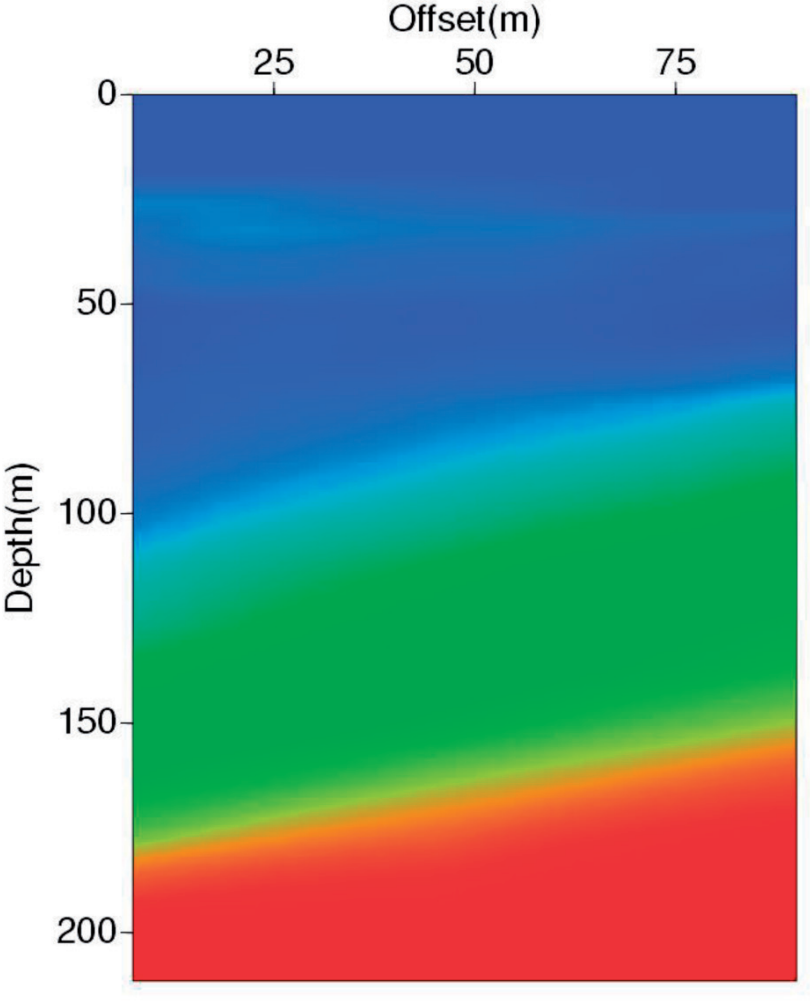

Figure 2: The smoothed version of Figure 1.

Fig. 2. The smoothed version of Fig. 1.

Figs. 3, 4 and 5 show the resultant synthetic shots corresponding to various frequency band widths of source wavelets. The source is located on the left side and 142 receivers are located at the right side. Each shot contains 142 traces and 1200 time samples. The trace interval is 1.5 m and the time sample rate is 0.2 ms.

The vertical and horizontal axes of Fig. 6 are time lag index and trace index respectively. There are three curves in this figure: the green curve is the cross-correlation based traveltime difference of Fig. 3(a) and Fig. 3(b); the red curve is the cross-correlation based travel-time difference of Fig. 4(a) and Fig. 4(b); the blue curve is the cross-correlation based traveltime difference of Fig. 5(a) and Fig. 5(b). It is apparent that with the increasing peak frequency of source wavelet, the shapes of corresponding seismic wave-fronts are changed, and the traveltime difference calculated by cross-correlation between observed and calculated seismic data are also changed.

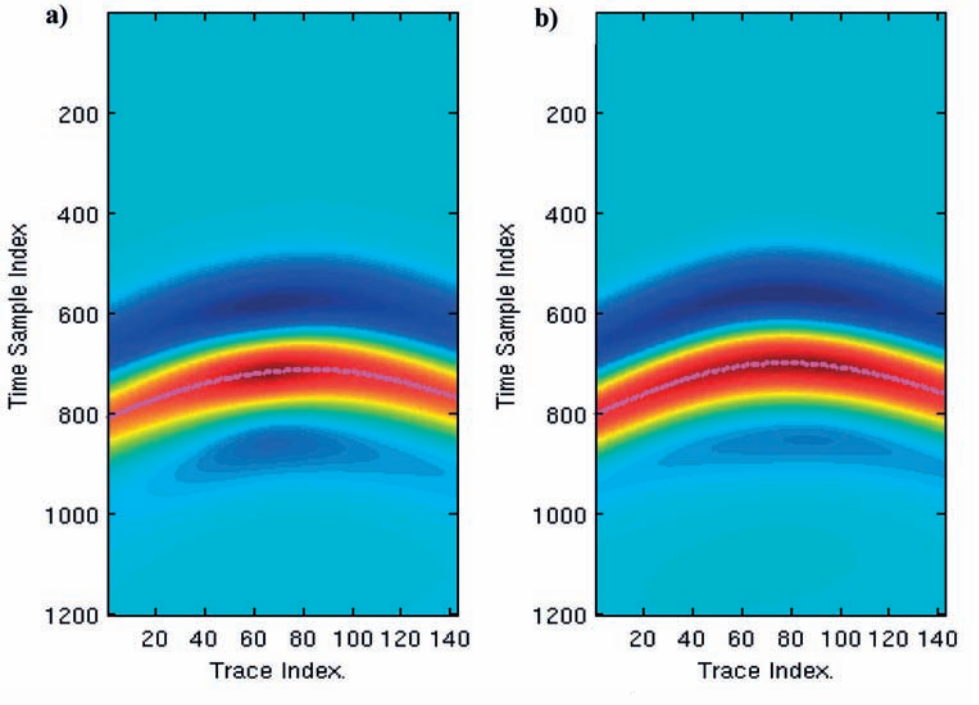

Fig. 3. Shot (a) is generated using the true velocity model shown in Fig. 1. Shot (b) is generated using the smoothed velocity model shown in Fig. 2. The source wavelets of shot (a) and (b) are 15 Hz Ricker wavelets. Each shot contains 142 traces and 1200 time samples. The trace interval is 1.5 m and the time sample rate is 0.2 ms.

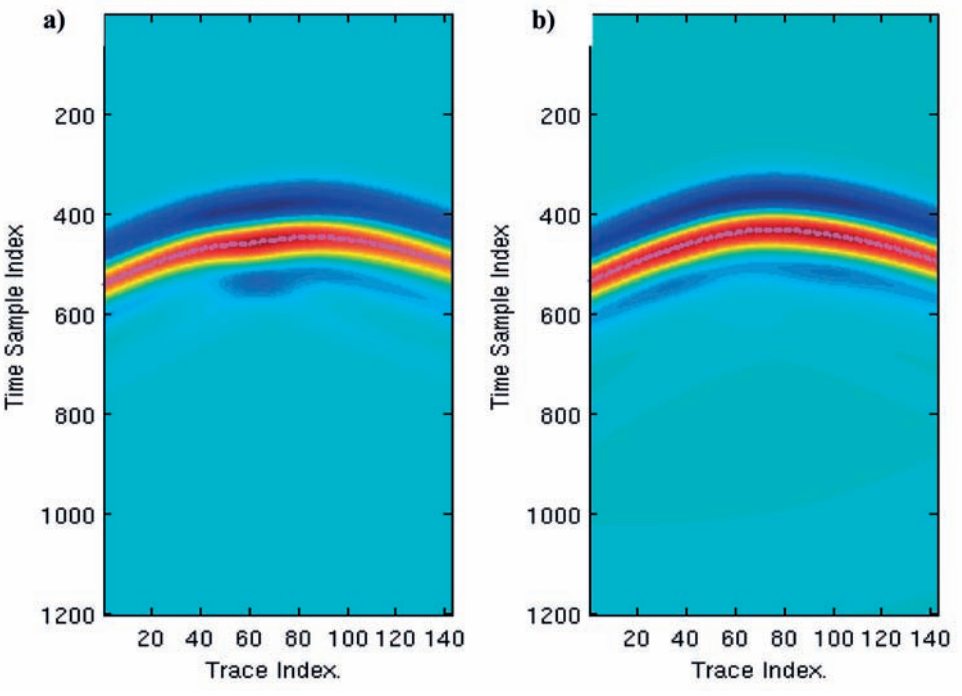

Fig. 4. Shot (a) is generated using the true velocity model shown in Fig. 1. Shot (b) is generated using the smoothed velocity model shown in Fig. 2. The source wavelets of shot (a) and (b) are 30 Hz Ricker wavelets. Each shot contains 142 traces and 1200 time samples. The trace interval is 1.5 m and the time sample rate is 0.2 ms.

NUMERICAL EXPERIMENTS

Wave equation traveltime inversion (WT) Example

We use Fig. 1 as a true velocity model and locate 18 sources on the left side and 36 receivers on the right side. The grid interval is 1.5 m and Fig. 7(a) shows the initial model which is constant at 3000 m/s. Fig. 7(b) is the WT inversion result after 18 iterations and the peak frequency of the source wavelet is 60 Hz. The inversion result successfully restores most characteristics of the true velocity model, but it is also obvious that there are many local minima exist in the inversion result and the resolution of inverted velocity still need to be improved.

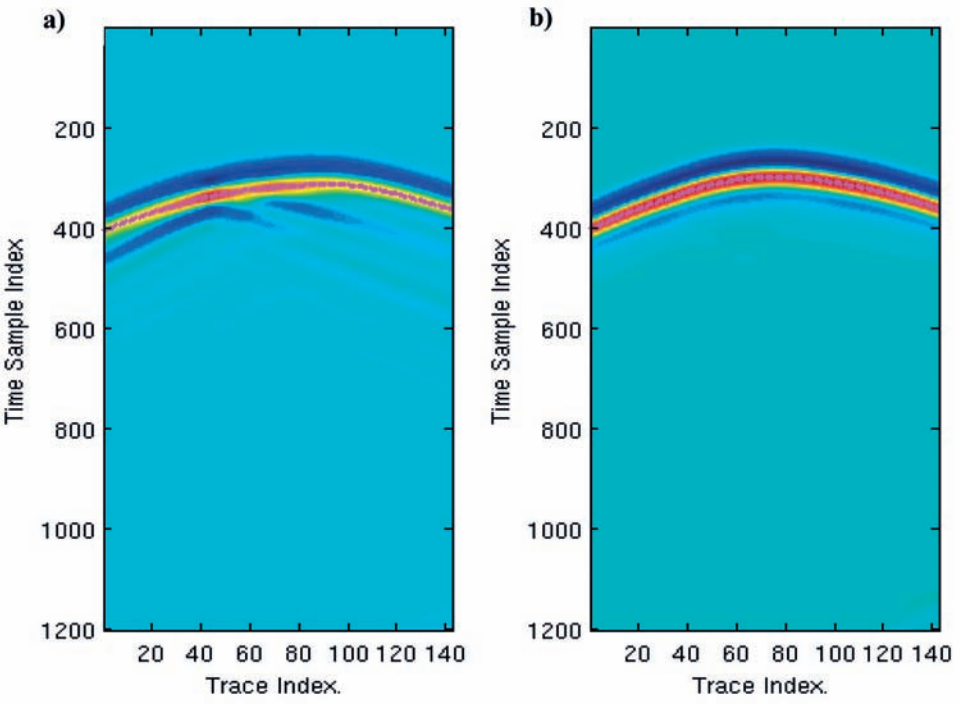

Fig. 5. Shot (a) is generated using the true velocity model shown in Fig. 1. Shot (b) is generated using the smoothed velocity model shown in Fig. 2. The source wavelets of shot (a) and (b) are 60 Hz Ricker wavelets. Each shot contains 142 traces and 1200 time samples. The trace interval is 1.5 m and the time sample rate is 0.2 ms.

Frequency-dependent wave equation traveltime inversion (FWT) example

The initial velocity model, true model and synthetic data used in FWT test are the same as in WT example. We first perform the inversion using low-passed data (peak frequency is 15 Hz), and then use the inversion result as another initial model and perform the inversion using a 30 Hz low-passed data, and finally do inversion using full frequency band. The FWT result after 30 iterations is shown in Fig. 7(c). Compared with WT result (as shown in Fig. 7(b)), it is obvious that FWT result has much higher resolution and contains less local minima, e.g., the fault boundaries are better delineated by FWT method. By using the FWT method, the smooth components of true velocity can be obtained, but if we want to invert the detailed sharp components, the FWI method should be used. It should be noted that the input frequencies can be reduced using frequency selection strategy (Sirgue and Pratt, 2003), which will improve the computational speed.

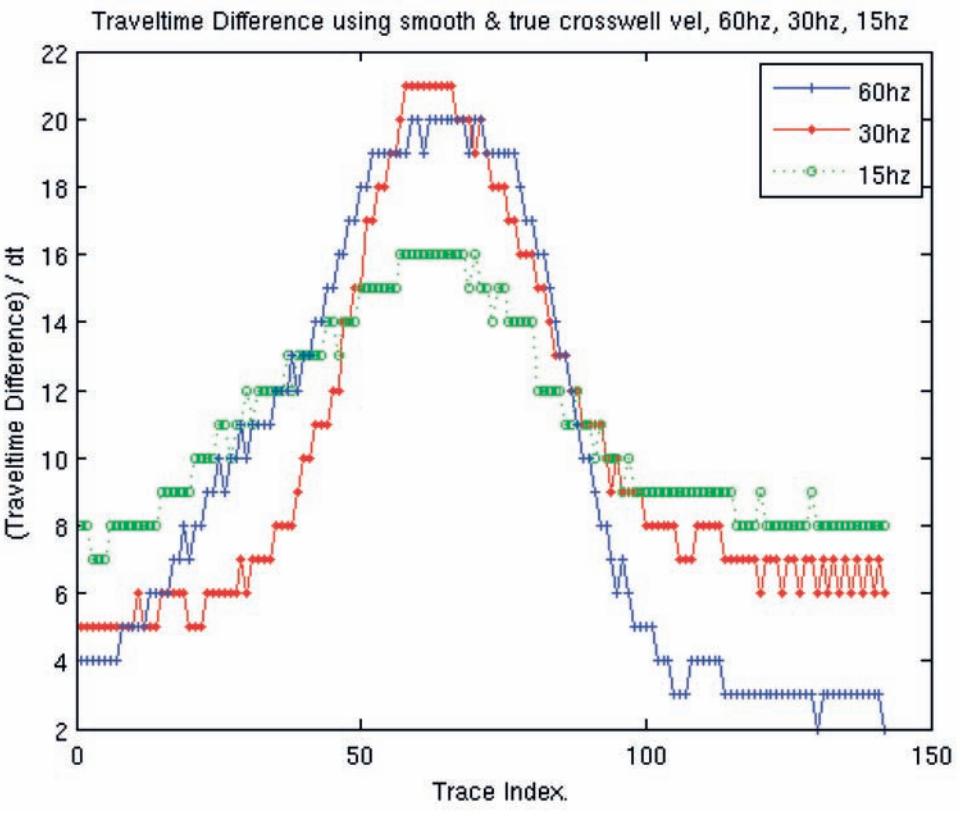

Fig. 6. The cross-correlation based travel-time difference of Fig. 3(a) and Fig. 3(b) is depicted in green. The travel-time difference of Fig. 4(a) and Fig. 4(b) is in red, and the blue shows the travel-time difference of Fig. 5(a) and Fig. 5(b). The horizontal axis represents the trace index and the vertical axis represents time lag index.

Full waveform inversion (FWI) example

We use Fig. 7(b) (WT result) as initial velocity model and apply conventional FWI using 60 Hz data, and the inverted velocity model after 6 iterations is shown in Fig. 8(a). We then use Fig. 7(c) (FWT result) as initial velocity model and apply conventional FWI again. The inverted velocity model after 6 iterations is shown in Fig. 8(b). The model misfits of Fig 7(b), Fig 7(c), Fig 8(a) and Fig 8(b) are 12.7%, 7.8%, 5.2% and 3.7%. It is clear that the resultant velocity model, shown in Fig. 8(b), is closest to the true velocity model. It means that the inversion flow of FWT followed by FWI produce the best result.

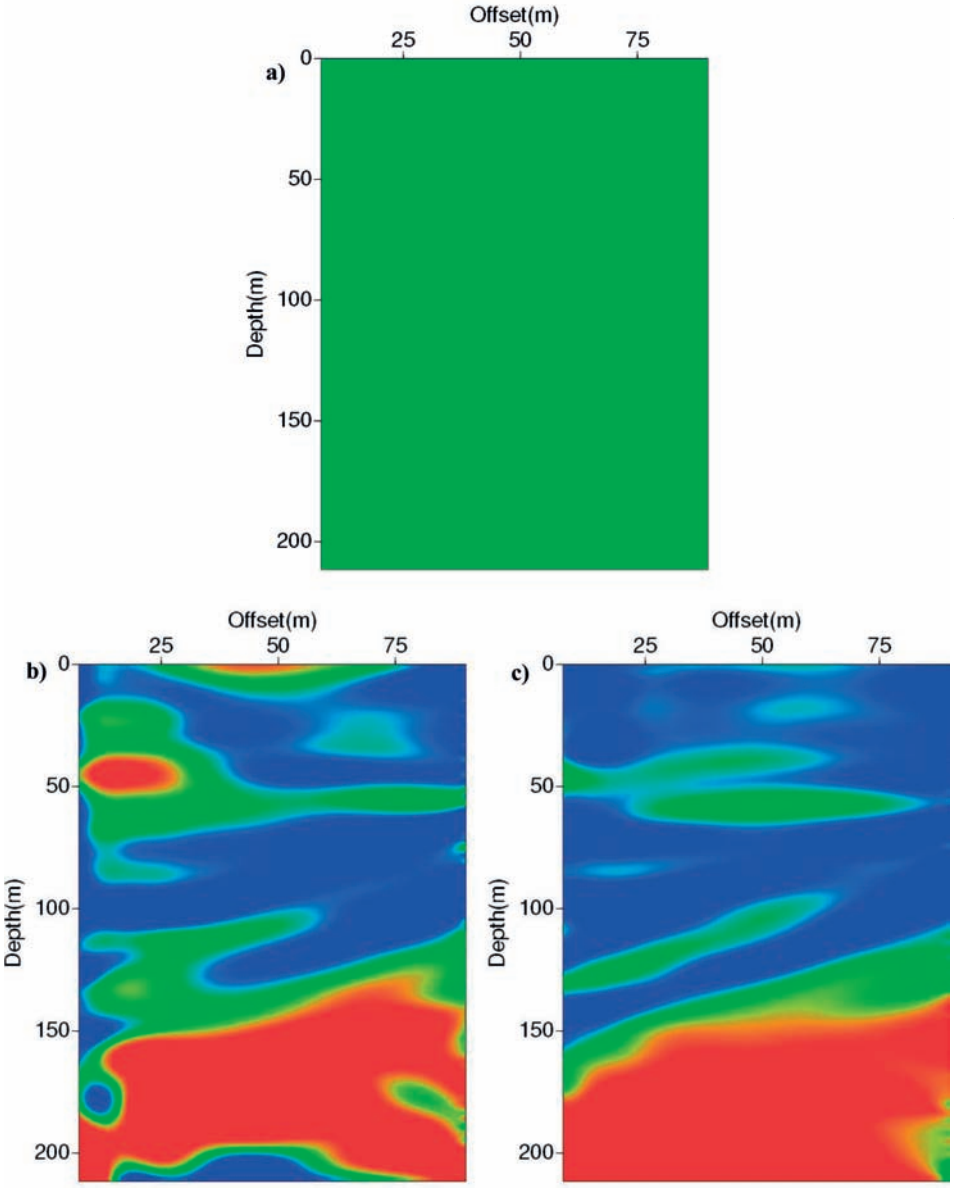

Fig. 7. (a) is the initial constant 3000 m/s velocity model, the grid interval is 1.5 m in both horizontal and vertical directions. (b) is the WT result using 60 Hz data and (c) is the FWT result using 15 Hz, 30 Hz and 60 Hz data.

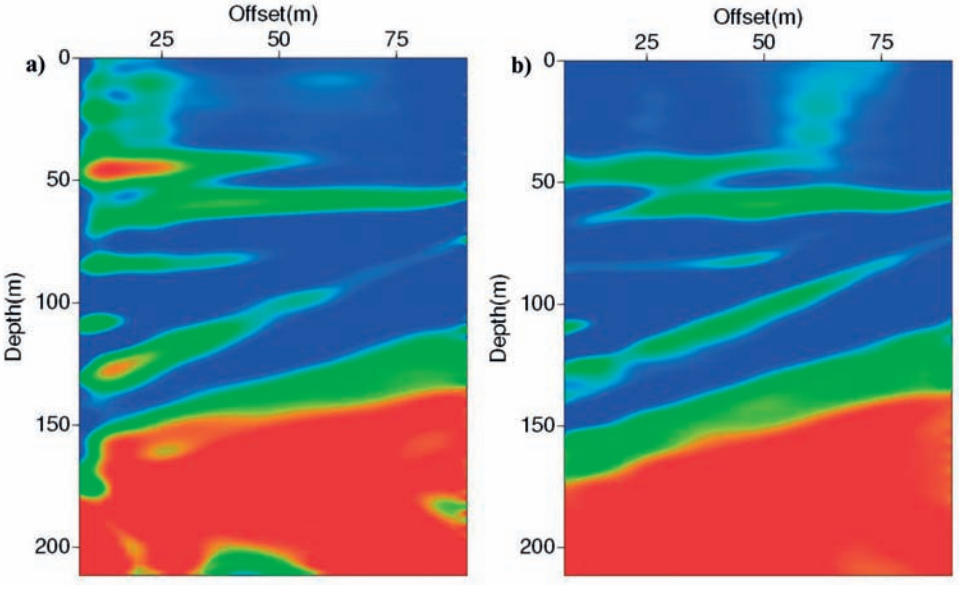

Fig. 8. (a) is waveform inversion result obtained by using the WT result (as shown in Fig. 7(b)) as initial velocity model; (b) is waveform inversion result obtained by using the FWT result (as shown in Fig. 7(c)) as initial velocity model.

CONCLUSION

In this paper a novel frequency dependent wave-equation traveltime inversion method, named FWT, is proposed. Its effectiveness and performance are shown with a synthetic cross-well dataset. Comparison with conventional WT inversion clearly indicates that the proposed FWT methodology can eliminate the local minima issues encountered in WT. Furthermore FWT provides a better initial velocity model than WT does for further refinement of the velocity estimations. An important message of this paper is that the FWT output is a much preferred input for subsequent FWI. Our future plans will be centered in the application of the FWT on field datasets as well as on refraction and diving wave data.

ACKNOWLEDGMENTS

The research was funded by the National Basic Research Program of China (973 Program, Grant No. 2011CB707303-ZT5), Science Foundation of Key Laboratory of Engineering Geomechanics, Institute of Geology and Geophysics, Chinese Academy of Sciences (No. KLEG201110), and the National Science and Technology Major Project of China (grant no. 2011ZX05030-004-001). We thank anonymous reviewers' constructive comments and thank Yi Luo, Tong Fei, Fuhao Qin and Panayotis G. Kelamis for discussions.

REFERENCES

Bishop, T., Bube, K., Cutler, R., Langan, R., Love, P., Resnick, J., Shuey, R., Spindler, D. and Wyld, H., 1985. Tomographic determination of velocity and depth in laterally varying media. Geophysics, 50: 903-923.

Crase, E., Wideman, C., Noble, M. and Tarantola, A., 1992. Nonlinear elastic waveform inversion of land seismic reflection data. J. Geophys. Res.: Solid Earth, 97: 4685-4703.

Dines, K.A. and Lytle, R.J., 1979. Computerized geophysical tomography. Proc. IEEE, 67: 1065-1073.

Gauthier, O., Virieux, J. and Tarantola, A., 1986. Two dimensional nonlinear inversion of seismic waveforms. Numerical results. Geophysics, 51: 1387-1403.

Ivansson, S., 1985. A study of methods for tomographic velocity estimation in the presence of low-velocity zones. Geophysics, 50: 969-988.

Luo, Y. and Schuster, G.T., 1991. Wave-equation traveltime inversion. Geophysics, 56: 645-653.

Mora, P., 1987. Nonlinear two-dimensional elastic inversion of multioffset seismic data. Geophysics, 52: 1211-1228.

Paulsson, B., Cook, N. and McEvilly, T., 1985. Elastic wave velocities and attenuation in an underground granitic repository for nuclear waste. Geophysics, 50: 551-570.

Shen, X., Tonellot, T., Luo, Y., Keho, T. and Ley, R., 2012. A new waveform inversion workflow: Application to near-surface velocity estimation in Saudi Arabia. Expanded Abstr., 82nd Ann. Internat. SEG Mtg., Las Vegas: 1-5.

Sirgue, L. and Pratt, R.G., 2003. Efficient waveform inversion and imaging: A strategy for selecting temporal frequencies. Geophysics, 69: 231-248.

Tarantola, A., 1984. Inversion of seismic reflection data in the acoustic approximation. Geophysics, 49: 1259-1266.

Tarantola, A., 1986. A strategy for nonlinear elastic inversion of seismic reflection data. Geophysics, 51: 1893-1903.

Zhang, S., Schuster, G.T. and Luo, Y., 2011. Wave-equation reflection traveltime inversion, SEG Expanded Abstr., 81st Ann. Internat. SEG Mtg., San Antonio: 2705-2710.

Zhou, C., Cai, W., Luo, Y., Schuster, G.T. and Hassanzadeh, S., 1995. Acoustic wave-equation traveltime and waveform inversion of crosshole seismic data. Geophysics, 60: 765-773.